Productive Entry of HIV-1 during Cell-to-Cell Transmission via Dynamin-Dependent Endocytosis

Richard D. Sloan,[a]* Björn D. Kuhl,[a,b] Thibault Mesplède,[a] Jan Münch,[c] Daniel A. Donahue,[a,d] Mark A. Wainberg[a,b,d]

McGill University AIDS Centre, Lady Davis Institute-Jewish General Hospital, Montreal, Quebec, Canada[a]; Division of Experimental Medicine, McGill University, Montreal, Quebec, Canada[b]; Institute of Molecular Virology, Ulm University, Ulm, Germany[c]; Department of Microbiology and Immunology, McGill University, Montreal, Quebec, Canada[d]

HIV-1 can be transmitted as cell-free virus or via cell-to-cell contacts. Cell-to-cell transmission between CD4$^+$ T cells is the more efficient mode of transmission and is predominant in lymphoid tissue, where the majority of virus resides. Yet the cellular mechanisms underlying productive cell-to-cell transmission in uninfected target cells are unclear. Although it has been demonstrated that target cells can take up virus via endocytosis, definitive links between this process and productive infection remain undefined, and this route of transmission has been proposed to be nonproductive. Here, we report that productive cell-to-cell transmission can occur via endocytosis in a dynamin-dependent manner and is sensitive to clathrin-associated antagonists. These data were obtained in a number of CD4$^+$ T-cell lines and in primary CD4$^+$ T cells, using both CXCR4- and CCR5-tropic virus. However, we also found that HIV-1 demonstrated flexibility in its use of such endocytic pathways as certain allogeneic transmissions were seen to occur in a dynamin-dependent manner but were insensitive to clathrin-associated antagonists. Also, depleting cells of the clathrin accessory protein AP180 led to a viral uptake defect associated with enhanced infection. Collectively, these data demonstrate that endosomal uptake of HIV-1 during cell-to-cell transmission leads to productive infection, but they are also indicative of a flexible model of viral entry during cell-to-cell transmission, in which the virus can alter its entry route according to the pressures that it encounters.

HIV-1 can be transmitted as free virus or directly between cells via cell-cell contacts. Cell-to-cell transmission is a more efficient and rapid means of viral spread and is the predominant mode of HIV-1 transmission in lymphoid tissue (1, 2). Given that the vast majority of virus within an infected individual is found in lymphoid tissue and in CD4$^+$ T cells, cell-to-cell transmission between CD4$^+$ T cells likely represents the most common mode of HIV-1 spread.

Improved understanding of the direct and coordinated interactions between T cells and antigen-presenting cells, termed immunological synapses (3), ultimately led to the first description of coordinated retroviral transmission between T cells. Human T-lymphotropic virus type I (HTLV-I) is transmitted via a polarized T-cell structure termed the virological synapse that is analogous to the immunological synapse (4). Subsequent studies revealed that HIV-1 could also be transmitted via virological synapses between CD4$^+$ T cells (5) and that infected cells could even form polysynapses, thereby allowing simultaneous cell-to-cell transmissions from a single infected cell to multiple uninfected target cells (6). Cell-to-cell transmission between infected macrophages and uninfected CD4$^+$ T cells has also been described (7). Further, a less common mode of transmission between CD4$^+$ T cells was shown to exist in which HIV-1 can be transmitted by long membrane nanotubes that are formed after cell division (8). A visually similar but mechanistically distinct process involving murine leukemia virus (MLV) was described in which virus can be transmitted in an actin-dependent manner along filopodial bridges that link cells (9, 10). Further, in striking intravital imaging experiments of HIV-1 infections in humanized mice, it was shown that infected lymphocytes were highly motile, leading to extensive viral spread, while infected lymphocytes formed cytoskeletal and membranous interactions with uninfected target cells (2). Finally, viral spread from virus-bearing, but not productively infected, dendritic cells to un-

infected CD4$^+$ T cells can also occur via direct cell-cell contacts and is an important contributor to viral spread and pathogenesis (11).

Of these processes, transmission via T-cell–T-cell virological synapses is one of the most studied (reviewed in references 12 and 13), yet many of the underlying cellular events are not well characterized. Early definition of the HIV-1 virological synapse revealed that transmission is dependent on extensive cytoskeletal rearrangements in both the donor and target cell (5, 14). Such transmission also requires lipid raft integrity (15), cell surface adhesion molecules (LFA-1, Talin, and ICAM-1) (16) and tetraspanins (CD63 and CD81) (17), tyrosine kinase signaling (ZAP-70) (18), and interactions between viral envelope glycoprotein gp120 and cellular CD4 (5). More recently, it has been shown that HIV-1 harnesses the regulated secretory pathways in CD4$^+$ T cells to achieve cell-to-cell transmission (19). Ultimately, transmission leads to virus egress into a synaptic cleft between the infected donor and the uninfected target cell, subsequently resulting in productive infection. This process is distinct from virus transmission mediated by cytoplasmic contacts between cells (13, 20).

Other mechanistic details are less clear, especially in regard to the endocytosis of viral particles by target cells involved in viro-

logical synapses. Live-microscopy analysis of virological synapses showed that green fluorescent protein (GFP)-fused HIV-1 Gag can traffic from the site of cell-cell contact to intracellular endosome-like structures in the target cell during transmission, with electron microscopy confirming the presence of viral buttons in the target cell (21). Notably, these structures were morphologically distinct from typical ligand-bearing clathrin-coated vesicles. Another study showed that disrupting endocytosis in target cells engaged in virological synapses inhibited uptake of viral p24 into cellular compartments bearing the early endosomal marker EEA1, but the relationship between this observation and productive infection remains unclear (22). This point is relevant since cell-free HIV-1 virions can commonly enter cells via nonproductive endocytic pathways (23). Equally, earlier studies of the virological synapse found no colocalization between HIV-1 Gag and EEA1 (5). More recently, virus-cell membrane fusion was described to occur in target cell endosomes during cell-to-cell transmission, a process that was dependent on protease-driven virion maturation (24).

The hypothesis of productive endocytic entry of HIV-1 during cell-to-cell transmission is consistent with prior observations of cell-free virus. Data from a variety of T-cell lines and primary CD4$^+$ T cells have shown that cell-free HIV-1 can productively enter cells in a dynamin-dependent manner via clathrin-mediated endocytosis (25–28). Indeed, a specific small-molecule antagonist of the clathrin terminal domain was found to antagonize HIV-1 entry into HeLa cells (29). However, in the stages leading to membrane fusion, cell-to-cell transmission appears to be mechanistically distinct from cell-free infection, so these findings may not be universally relevant. Additionally, some studies used transmission electron microscopy (TEM) to analyze cell-to-cell transmission via virological synapses and found no evidence of HIV-1 within target cell endosomes, instead showing virus exclusively in the synaptic cleft between donor and target cell (20). At present, the reasons for such major discrepancies between these studies are unclear. Yet given that HIV-1 can usurp CD4$^+$ T-cell specific secretion pathways (19) and that immunological synapses are characterized by high rates of endocytic and exocytic turnover (30), it is reasonable to hypothesize that HIV-1 may have evolved to use endocytic processes as a means of attaining productive cell-to-cell infection in some circumstances. Given these discrepancies, we wanted to better characterize the role of target cell endocytic pathways in productive cell-to-cell HIV-1 transmission. Therefore, we have asked whether the visually apparent endosomal viral uptake routes that are found during cell-to-cell transmission can genuinely lead to productive infection of the target cell.

To achieve this, we probed the viral entry cascade during cell-to-cell transmission with antiviral drugs to establish that events downstream of CD4 binding can occur from within target cell compartments, consistent with an endosomal entry mode. Using both small-molecule inhibition and RNA interference (RNAi), we now demonstrate the pivotal role of the membrane-bound GTPase dynamin-2 in productive infection. Further, we show the involvement of the endocytic uptake in productive cell-to-cell transmission. Interestingly, we also observed that the use of endocytic entry routes by virus is not always apparent as transmission of virus via a clathrin-associated antagonist-sensitive route was rendered dysfunctional during some allogeneic CD4$^+$ T-cell transmissions. Our findings suggest a model of cell-to-cell transmission via virological synapses that is inherently flexible between both endocytic and other transmission modes, allowing HIV-1 to alter its entry route according to infection conditions and the pressures it encounters during transmission.

MATERIALS AND METHODS

Cells. The CD4$^+$ T-cell lines PM1, SupT1, and Jurkat (clone E6-1) were obtained via the NIH AIDS Research and Reference Reagent Program. These lines were maintained in RPMI 1640 medium (Invitrogen). 293T cells were maintained in Dulbecco modified Eagle medium (DMEM) (Invitrogen). All cell lines were maintained with 10% fetal bovine serum (FBS), 1% L-glutamine, and 1% penicillin-streptomycin.

Peripheral blood mononuclear cells (PBMCs) were isolated from whole blood using the Ficoll-Hypaque method. CD4$^+$ T cells were purified from PBMCs by negative selection using the CD3$^+$ CD4$^+$ Untouched kit (Invitrogen) commonly giving ~90% purity. CD4$^+$ T cells were cultured in RPMI 1640 medium supplemented with 20 U/ml human interleukin-2 (IL-2). CD4$^+$ T cells were activated with either 10 μg/ml phytohemagglutinin A (PHA) for 72 h or with anti-CD3/anti-CD28 Dynabeads (Invitrogen) for 48 h. Cells were then either pooled or were maintained separately for autologous transmissions.

Viruses. The NL4-3-derived viral clone pBR-NL43-IRES-eGFP or its derivatives were used to produce virus for infections (31). This clone expresses green fluorescent protein (GFP) from an internal ribosomal entry site (IRES) downstream of Nef. The V3 loop from the envelope of the primary R5-tropic molecular clone YU2 was cloned into pBR-NL43-IRES-eGFP. Virus was produced by plasmid lipofection (Invitrogen) into 293T cells, harvested 72 h later, clarified by low-speed centrifugation, and passed through a 0.45-μm-pore-size filter. Viral p24 levels were quantified by a Vironostika HIV-1 antigen (Ag) enzyme-linked immunosorbent assay (ELISA) kit (bioMérieux).

Antiviral drugs and endocytosis inhibitors. The antivirals maraviroc, AMD3100, and T-20 as well as the anti-CD4 monoclonal antibody B4 and soluble CD4 were all obtained via the NIH AIDS Research and Reference Reagent Program. BMS-599793 was provided by the International Partnership for Microbicides (IPM). Chlorpromazine, dynasore, bafilomycin A1, and latrunculin A1 were obtained from Sigma. MiTMAB (tetradecyltrimethylammonium bromide) was obtained from Tocris.

RNA interference. The isopropyl β-D-1-thiogalactopyranoside (IPTG)-inducible vector pLKO-IPTG-3xLacO (Sigma) was used to express short hairpin RNAs (shRNAs) targeted against human dynamin-2 and human AP180 (Sigma Mission TRCN0000006649 for dynamin-2 and TRCN0000119072 for AP180). Additionally, a nontarget (scramble) control was also prepared. Viral particles for cell line transductions were prepared by cotransfecting 293T cells with pLKO-IPTG-3xLacO, the Gag/Pol expression vector PsPAX, a Rev expression vector, and the vesicular stomatitis virus G protein (VSV-G) expression vector pVPack-VSV-G (Stratagene). After 48 h, virus was clarified by low-speed centrifugation and passed through a 0.45-μm-pore-size filter. Viral p24 levels were quantified by a Vironostika HIV-1 Ag ELISA kit (bioMérieux).

PM1 and Jurkat cells were transduced by culturing viral particles in the presence of 8 μg/ml Polybrene for 72 h, after which resistant colonies were selected with 2 μg/ml puromycin. Transduced wells were maintained in 0.5 μg/ml puromycin except during coculture experiments, during which transduced cells were cultured without puromycin for 24 h prior to coculture. Culturing cells in the presence of 1 mM IPTG for 72 h induced expression of shRNAs.

Intracellular protein staining. Dynamin-2 and AP180 levels in PM1 cells and Jurkat cells were assayed by flow cytometry. Cells were fixed in 1% paraformaldehyde–phosphate-buffered saline (PBS) and then permeabilized using a saponin-containing Wash/Perm solution (BD Bioscience). Cells were stained in PBS containing 3% bovine serum albumen (BSA) and 0.05% sodium azide with rabbit anti-dynamin-2 polyclonal Cy5-conjugated antibodies (Bioss) or goat polyclonal anti-AP180 (Abcam). Thereafter, anti-AP180-treated cells were stained with rabbit anti-goat IgG peridinin chlorophyll protein (PerCP)-conjugated polyclonal

antibodies (Santa Cruz Biotechnology). Samples were then read on a FACSCalibur flow cytometer (BD) collecting 10,000 live events.

Cell-to-cell transmission assays. We used a previously established flow cytometry-based assay to determine rates of viral p24 transfer and GFP expression in target cells during cell-to-cell transmission (32). A total of 1×10^6 PM1 cells or Jurkat cells were infected with 93.75 ng and 187.5 ng of viral p24, respectively, via spinoculation at $1,500 \times g$ for 2 h at 37°C, followed by 1 h of incubation at 37°C. Primary CD4^{+} T cells were infected by spinoculation also, using 100 ng per 10^6 cells in the presence of 8 µg/ml Polybrene. At 72 h after infection (or 48 h for primary cells), cells were washed and stained with either 10 µM Cell Tracker Blue (CMAC; 7-amino-4-chloromethylcoumarin) (Molecular Probes) or 2.5 µM Cell Tracker Violet [BMQC; 2,3,6,7-tetrahydro-9-bromomethyl-1H,5H-quinolizino(9,1-*gh*)coumarin] (Molecular Probes) for 30 min. Target cells that were pretreated with antivirals (either 5 µM maraviroc, 5 µM AMD3100, 5 µM T-20, or 5 µM BMS-599793) were pretreated for 1 h prior to coculture with infected cells, and drug concentrations were maintained throughout the coculture period. In experiments to study endocytic pathways, target cells were pretreated with endocytosis inhibitors for 45 min (either 80 µM dynasore, 0.45 M sucrose, 100 nM bafilomycin A1, or 10 or 2 µg/ml chlorpromazine) before being washed out, except for 80 µM MiTMAB which was used for 30 min. Treated cells were then used in coculture. For RNAi experiments, shRNAs were induced in Jurkat and PM1 cells for 72 h prior to coculture using 1 mM IPTG that was maintained throughout coculture experiments to maintain shRNA expression. For infection, washed donor cells were mixed with stained target cells at a 2:1 ratio. For autologous transmissions using primary CD4^{+} cells, cells were infected and mixed with uninfected stained target cells from the same blood donor in a 3:1 ratio. In all experiments transwell inserts (3-µm pore size; Nunc) were used to control for cell free infection.

Transfer of virus from infected donor cells to uninfected target cells was shown by intracellular staining for viral p24 in the target cell population. In experiments with antivirals this was at 6 h after coculture. In experiments with endocytosis inhibitors or RNAi, this was at 3 h after coculture. Cells were fixed in 4% paraformaldehyde-PBS, permeabilized using a saponin-containing Wash/Perm solution (BD Bioscience), and then stained with anti-p24-conjugated phycoerythrin (PE) (Beckman Coulter) in PBS containing 3% BSA and 0.05% sodium azide. In some instances, cells were pretreated with 0.25% trypsin for 8 min at 37°C before being quenched in cold FBS, prior to staining. Infection of target cells was detected by GFP expression at 24 h postcoculture, at which time cells were fixed in 4% paraformaldehyde-PBS.

Samples stained with Cell Tracker blue (CMAC) were analyzed using an LSRII instrument (Becton, Dickinson) or a fluorescence-activated cell sorter (FACS) Vantage instrument (Becton, Dickinson) while samples stained with Cell Tracker violet (BMQC) were analyzed on an LSR Fortessa (Becton, Dickinson). Single cells only were assayed by gating on both forward scatter width and side scatter width parameters. Equally, p24 and GFP levels were assayed only in cells with high cell tracker expression. Therefore, cell populations in which cell tracker strength had been diluted either by cell-cell fusion or cell division could be excluded (5). A minimum of 20,000 to 50,000 live cell events were collected. Experiments were analyzed with FlowJo software (Tree Star). A minimum of three independent experiments with duplicate infections were performed.

Cell surface receptor staining. PM1 and Jurkat cells that had been treated to inhibit endocytosis were stained for cell surface CD4 and CXCR2 2 h afterwards. Cells were stained in 3% fetal bovine serum and 0.05% sodium azide for 30 min at 4°C with mouse monoclonal allophycocyanin (APC)-conjugated anti-human CD4 (clone RPA-T4; BD PharMingen) and mouse monoclonal PE-conjugated anti-human CXCR4 (clone 12G5; BD PharMingen). Cells were then fixed in a final concentration of 1% paraformaldehyde and then resuspended in PBS containing 3% fetal bovine serum and 0.05% sodium azide. A total of 10,000 live cell events were assayed on a FACSCalibur (Becton, Dickinson) instrument. Levels of receptors were quantified relative to those

found for dimethyl sulfoxide (DMSO)-treated cells. Experiments were analyzed with FlowJo software (Tree Star).

Cellular viability staining. PM1, Jurkat, and SupT1 cells or pooled anti-CD3/anti-CD28-activated primary CD4^{+} T cells were pretreated with drugs to inhibit endocytosis. Cells were then stained with a Green Live/Dead cell viability stain (Invitrogen) according to the manufacturer's instructions. As a control, heat-killed cells (65°C for 7 min) were assayed. Cells were fixed in 4% paraformaldehyde, and 10,000 events were analyzed on a FACSCalibur (Becton, Dickinson) flow cytometer.

Statistical analysis. The results presented are derived from a minimum of three independent experiments performed in duplicate at minimum. Data were analyzed using GraphPad Prism, version 5, software. Differences between two treatments were tested for statistical significance using unpaired two-tailed *t* tests. Differences between treatment groups were tested using one-way analysis of variance (ANOVA) using Dunnett's posttest to compare treatment groups with control data. The results presented are expressed as means ± standard errors of the means (SEM).

RESULTS

Virus coreceptor binding and virus-cell membrane fusion occur from within target cells during cell-to-cell transmission. We first wished to determine the fate of virus during cell-to-cell transmission when the viral entry cascade was inhibited at discrete points through the use of specific antiviral agents targeting various steps in the viral life cycle. We used a previously developed flow cytometry cell-to-cell transmission assay using an HIV-1 NL4-3-based GFP reporter virus that coexpresses *nef* and the fluorescence protein from a bicistronic RNA (31, 32). Infected washed donor cells were mixed with cell tracker-labeled target cells (either BMQC-violet or CMAC-blue), and viral transfer into target cells was assayed at 6 h after coculture by measuring intracellular p24. This time point was chosen to exclude *de novo* synthesis of viral p24 in the target cells, such that all p24 present would have occurred from the transfer of virus from donor into target cells. This was confirmed by treating cocultured cells with a 5 µM concentration of the integrase inhibitor raltegravir prior to and during coculture (data not shown). Cells were also treated with trypsin in some instances, allowing cell surface-associated p24 to be removed in order to assay only cellular uptake of p24 into trypsin-resistant compartments, which may be considered to be either endosomal vesicles or the cytosol (1, 33).

This dual format allowed us to distinguish between the transfer of viral proteins into target cells (p24) and viral transmission, in which integrated virus would lead to expression of virus-borne genes (GFP). In this study, as with others, we have taken virus-borne GFP expression to be a measure of infection (34, 35). Alternative methods to study cell-to-cell transmission are possible and rely on the use of reverse transcriptase (RT) inhibitors to inhibit *de novo* DNA or p24 synthesis, thereby providing control data for DNA or p24 accumulation in the coculture. Viral DNA accumulation or p24 accumulation is then used as a proxy for successful cell-to-cell transmission. We chose not to perform such an analysis as we have previously shown this approach to be less precise than our assay (32).

As a control for cell-free virus infections, transwell inserts with a 3-µm pore size were used to prevent cell-cell contacts yet allow free movement of virus between donor and target cell populations. Under these circumstances, neither p24 nor GFP was detected at 6 h or 24 h, respectively (data not shown). This confirms that our coculture model assayed only cell-to-cell transmission as the viruses found in supernatants arising from washed donor cells
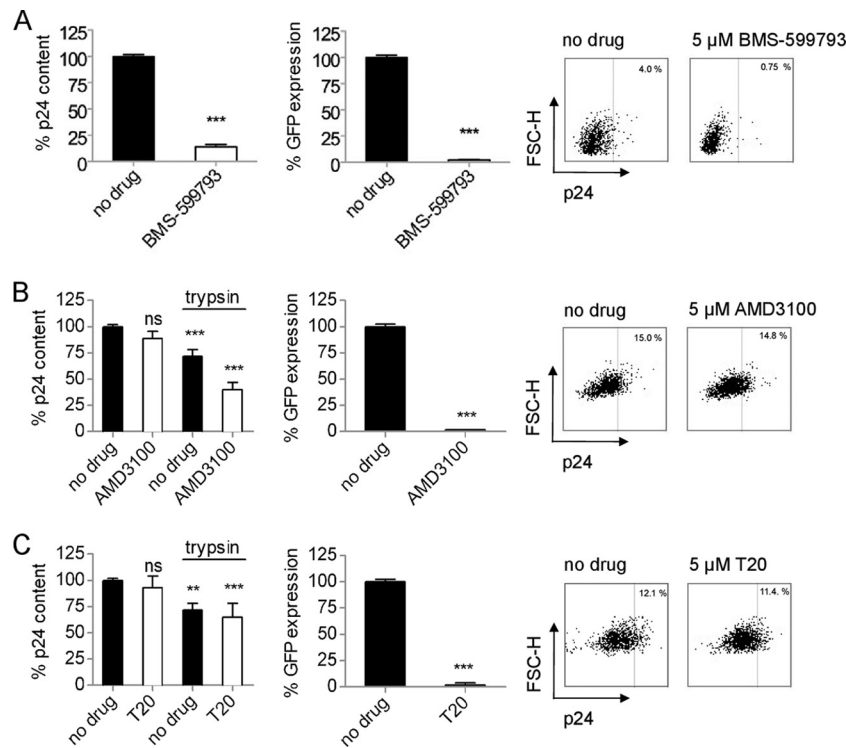
FIG 1 Antagonizing HIV-1 entry downstream of CD4 binding during cell-to-cell transmission fails to prevent viral transfer to target cells. (A) Relative p24 content or reporter virus GFP expression of target cells during cell-to-cell transmission between PM1 cells using X4-tropic NL4-3-derived virus. gp120-CD4 binding was antagonized with the small-molecule gp120 inhibitor BMS-599793. Representative flow cytometry data are shown. (B) Relative p24 content or reporter virus GFP expression of target cells during cell-to-cell transmission. Coreceptor binding was antagonized with the CXCR4 antagonist AMD3100. In some instances cells were treated with trypsin prior to analysis. Representative flow cytometry data are shown. (C) Relative p24 content or reporter virus GFP expression of target cells during cell-to-cell transmission. Virus-cell membrane fusion was antagonized by the fusion inhibitor T-20, and cells were treated with trypsin prior to analysis. Representative flow cytometry data are shown. All data are means ± SEM ($n \geq 3$); statistically significant results are indicated with asterisks; not significant (ns), $P > 0.05$, *, $P \leq 0.05$; **, $P \leq 0.01$; ***, $P \leq 0.001$; ****, $P \leq 0.0001$. FSC, forward scatter.

were unable to yield productive infection in target cells during this time frame.

To exclude transmission of virus via cell-cell fusion events (i.e., syncytium formation) rather than via virological synapses, our flow cytometry analyses excluded all particles detected as doublets or larger by gating based on both forward scatter and side scatter pulse width, which restricted our analysis only to particles of single-cell size. Additionally, as fusion between cell tracker-stained target cells and unstained target cells might result in a particle with diluted cell tracker content (5), we excluded such cells from our analysis. This therefore also excluded transmission events via membrane nanotubes as this mode of transmission, though less common, occurs when membrane filaments extend between recently divided cells (8). As cell tracker-stained cells that have divided would also have reduced cell tracker content, transmission via membrane nanotubes would not be measured in our assay. Equally, non-cell tracker-stained cells that have divided and are engaged in transmission via membrane nanotubes would not be measured as our analysis was based on cell tracker-stained cells only. Thus, while measuring bulk cell-to-cell transmission in coculture infections, our gating strategy allowed analysis only of transmission via virological synapses, the predominant mode of cell-to-cell transmission (1).

Previous analyses have suggested that coreceptor binding and membrane fusion may not occur at the cell surface during cell-to-

cell transmission (24, 36). However, these findings remain contentious, and so we wished to explore this dichotomy in our own analysis. We first investigated transmission between PM1 cells, in which donor PM1 cells that had been infected for 72 h (the infection was 10 to 25% positive by GFP) were used to infect cell tracker-stained target PM1 cells at a 2:1 ratio. We sought to inhibit viral gp120 binding to cellular CD4 using a small molecular inhibitor of gp120, BMS-599793. Cells were pretreated for 1 h with a fully inhibitory 5 μM concentration of BMS-599793 (37), which was maintained throughout the coculture period. That no detectable GFP expression was found in the target cell population after 24 h confirmed that inhibition had occurred (Fig. 1A). Equally, the vast majority (86%) of target cells treated with BMS-599793 had no detectable p24 after 6 h of coculture (Fig. 1A). Therefore, although very effective, even high concentrations of BMS-599793 may not be able to completely inhibit all viral transfer to target cells. These data confirm previous observations that cell-to-cell viral transmission and initiation of HIV-1 infection are dependent on gp120-CD4 interactions (5, 36).

We next asked whether antagonizing the viral entry cascade downstream of CD4 binding would yield similar results. We performed coculture experiments using a 5 μM concentration of the CXCR4 antagonist AMD3100, which could fully inhibit infection by a CXCR4-tropic reporter virus (Fig. 1B). Some infection models have suggested that such inhibition might fail to prevent trans-

fer of viral protein into target cells (36). Our data show that blockage of CXCR4 binding had no significant effect on the total p24 content of target cells even though 5 μM AMD3100 completely prevented GFP expression in target cells (Fig. 1B). As some target cell p24 content may derive from surface-bound virus (1), we also performed additional experiments in which cells were treated with trypsin prior to p24 staining and showed that 40% of AMD3100-treated target cells possessed detectable p24 levels relative to no-drug controls and that 56% possessed p24 relative to trypsin-treated drug controls. Thus, blockage of HIV-1 entry at the point of coreceptor binding during cell-to-cell transmission was not able to completely prevent viral transfer into trypsin-resistant compartments in target cells. Our data also suggest that a degree of coreceptor binding (44%) can occur at the cell surface in our PM1 cell-to-cell transmission model.

We next investigated whether antagonizing the viral entry cascade downstream of coreceptor binding, at the point of virus-cell membrane fusion, would yield similar results. Target cells were incubated with the fusion antagonist T-20 (5 μM) both before and during coculture infections. As with the blockage of coreceptor binding, T-20 was not able to prevent viral transfer to target cells despite fully inhibiting infection (Fig. 1C). When cells were treated with trypsin, there was still no significant difference between control cells and T-20-treated cells (Fig. 1C). If the site of action for T-20 is the cell surface, this would decrease p24 uptake into the cytosol, a phenomenon that would be manifest in our results as reduced uptake into trypsin resistant compartments. The fact that no such inhibition was observable suggests that no virus-cell membrane fusion events occurred at the cell surface and that all virus-cell membrane fusion events likely occurred from within trypsin-resistant compartments in target cells during cell-to-cell transmission. This finding confirms our PM1-based analysis with studies of Jurkat cells and primary cells (24).

Dynamin-dependent cell-to-cell transmission of HIV-1. Our initial analysis suggested that just over half of coreceptor binding and all membrane fusion during cell-to-cell transmission can occur from within trypsin-resistant compartments in target cells. We hypothesized that virus enters into endocytic vesicles within target cells, in which the events of the entry cascade downstream of CD4 binding might unfold. Given parallels between this hypothesis and prior descriptions of entry of cell-free HIV-1 via endocytosis (25, 28), we also investigated the role of the host cell GTPase dynamin-2 in cell-to-cell transmission. Dynamin mediates endocytic vesicle scission, allowing vesicles to pinch off from the cell surface and modulate membrane fusion. Therefore, dynamin is an important component of clathrin-mediated endocytosis, caveolar endocytosis, and other noncanonical endocytic processes (38).

Utilizing our flow cytometry assay of cell-to-cell transmission between PM1 cells, we determined the role of dynamin through pretreatment of target cells by the small-molecule dynamin antagonists (dynasore and MiTMAB) or by using an shRNA directed against dynamin. We then measured p24 uptake and GFP expression in target cells at 3 h and 24 h postcoculture, respectively.

Antagonism of dynamin by a 45-min pretreatment of target cells with 80 μM dynasore led to a modest but significant and reproducible 21% reduction of uptake of viral p24 by target cells (Fig. 2A). Furthermore, viral GFP expression in target cells was found to be reduced by 30% at 24 h after drug washout (Fig. 2B). When trypsin treatment of cocultured cells was performed, a

more potent effect of dynasore was noted, leading to 44% less p24 in target cells than in controls (Fig. 2A). It should also be noted that studies on antagonism of dynamin using dynasore have generally not revealed any decrease in cell surface levels of CD4, CXCR4, and CCR5 (22, 25, 28, 39, 40), and this was confirmed for CD4 and CXCR4 in our assays on both PM1 and Jurkat cells (Fig. 2C; see also Fig. 6D). Although some studies have described apoptosis in HeLa cells during extended exposure to some dynamin inhibitors (41), cellular viability staining indicated that the dynasore concentrations and conditions used were not cytotoxic in PM1 or any other cells studied, nor were other endocytosis inhibitors that were studied (Fig. 2F; see also Fig. 6H and 7C).

Other investigators have noted an increased potency of dynasore when cells are preincubated with this drug in the absence of fetal bovine serum (FBS) (39, 40). In our system, such pretreatment yielded an 82% inhibition (~5-fold) of viral p24 uptake into trypsin-resistant compartments and a 31% reduction in GFP expression compared to untreated controls (Fig. 2A and B). However, we did find that a portion of this antagonism was associated with the absence of FBS (Fig. 2A).

MiTMAB is a dynamin antagonist that is chemically distinct from dynasore (42), giving us the opportunity to investigate cell-to-cell transmission while minimizing potential artifactual results due to off-target effects associated with dynasore only. We found that pretreatment of PM1 cells with 80 μM MiTMAB prior to coculture yielded a 32% reduction of viral p24 uptake in target cells and a 38% reduction of viral GFP expression in target cells after coculture transmission (Fig. 2). Strikingly, when MiTMAB-treated target cells were also trypsin treated to exclude cell surface staining, we again found a ~5-fold reduction in target cell p24 uptake. These results, combined with those on dynasore treatment in the absence of FBS, imply that almost all target cell uptake of virus is due to dynamin-dependent processes, and this was linked in all instances to a reduction of productive infection as measured by GFP (Fig. 2).

To confirm the above data by genetic analysis, PM1 cells were transduced with inducible lentiviral vectors that expressed either scrambled control shRNAs or an shRNA targeting human dynamin-2. After 72 h of induction, the shRNA was found to yield a ~40% reduction of intracellular dynamin-2 levels in both groups of PM1 cells (Fig. 2E). This allowed us to perform flow cytometry-based cell-to-cell transmission assays using PM1 cells that expressed an anti-dynamin shRNA as target cells, yielding a >2-fold reduction in both target cell p24 uptake and target cell reporter virus GFP expression (Fig. 2D), a level that is similar to the degree of dynamin knockdown achieved. Dynamin depletion by shRNA gave results in which the p24 uptake and infection (i.e., GFP expression) were generally similar, unlike the use of dynasore and MiTMAB, which produced a 5-fold inhibition of p24 uptake but a more modest inhibition of infection (31% and 38%, respectively). This pattern was expected and was likely due to the drugs being washed out prior to analysis, producing a potent phenotype at the 2-h time point when p24 is assayed, versus the 24-h time point when GFP is assayed and drug levels are much diminished. In contrast, anti-dynamin-2 shRNAs were induced throughout the experiment, giving more similar p24 and GFP data. Overall, the shRNA data confirm our results with the small-molecule inhibitors dynasore and MiTMAB and demonstrate that dynamin-dependent uptake of HIV-1 is involved in cell-to-cell transmission and productive infection.
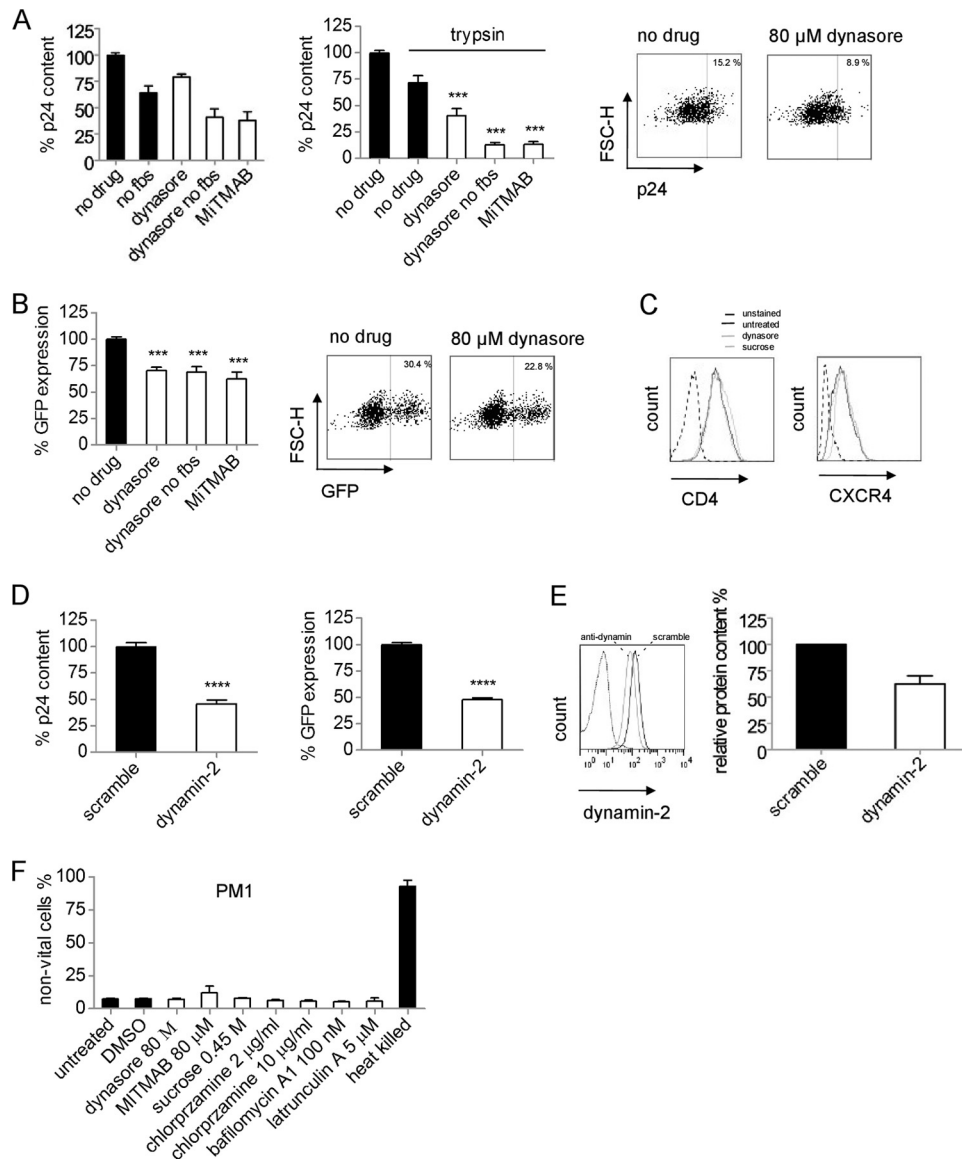
FIG 2 Association between dynamin function, virus transfer into target cells, and productive infection during cell-to-cell transmission. (A) Relative p24 content of target cells during cell-to-cell transmission between PM1 cells using X4-tropic NL4-3-derived virus and antagonism of dynamin function by pretreatment of target cells with the small-molecule antagonist dynasore (with or without FBS) or the dynamin antagonist MiTMAB. In some instances cells were treated with trypsin prior to analysis. Representative flow cytometry data are shown. (B) Relative reporter virus GFP expression of target cells during cell-to-cell transmission. Dynamin function was antagonized by pretreatment of target cells with the small-molecule antagonist dynasore (with or without FBS) or the dynamin antagonist MiTMAB. Representative flow cytometry results are shown. (C) Expression of cell surface CD4 or CXCR4 on PM1 cells 2 h following dynasore or hypertonic sucrose treatment. Representative histograms are shown. (D) Relative p24 content or reporter virus GFP expression of target cells during cell-to-cell transmission. Dynamin-2 levels were depleted in target cells via the expression of an shRNA directed against it. Representative flow cytometry results are shown. (E) Confirmation of dynamin-2 knockdown in PM1 cells via shRNA expression. shRNAs were expressed via transduction and IPTG induction. Intracellular staining by flow cytometry confirmed knockdown; a representative histogram and mean data are shown. (F) Cellular viability of PM1 cells following treatment with endocytosis inhibitors relative to heat-killed cells. All data are means ± SEM ($n \geq 3$); statistically significant results relative to controls (black columns) are indicated.

Productive cell-to-cell transmission of HIV-1 is sensitive to clathrin-associated antagonists. Dynamin-dependent endocytic vesicle scission is predominantly associated with the uptake of endocytic vesicles via clathrin-mediated endocytosis or via caveolae. Since human lymphocytes, including $CD4^+$ T cells, do not express the protein caveolin-1 (cav-1) or bear caveolae (39, 43–47), we next wanted to investigate whether the dynamin dependence of target cell virus transfer and productive infection that we

observed was due to clathrin-mediated, dynamin-dependent endocytosis (38, 48). We employed a mix of small-molecule inhibitors of this process and shRNAs directed to the clathrin accessory protein AP180.

We pretreated cell tracker-stained target PM1 cells with chlorpromazine, a small-molecule inhibitor of clathrin-mediated endocytosis that is thought to function by causing the heterotetrameric coat assembly complex AP2 to dissipate away from the cell
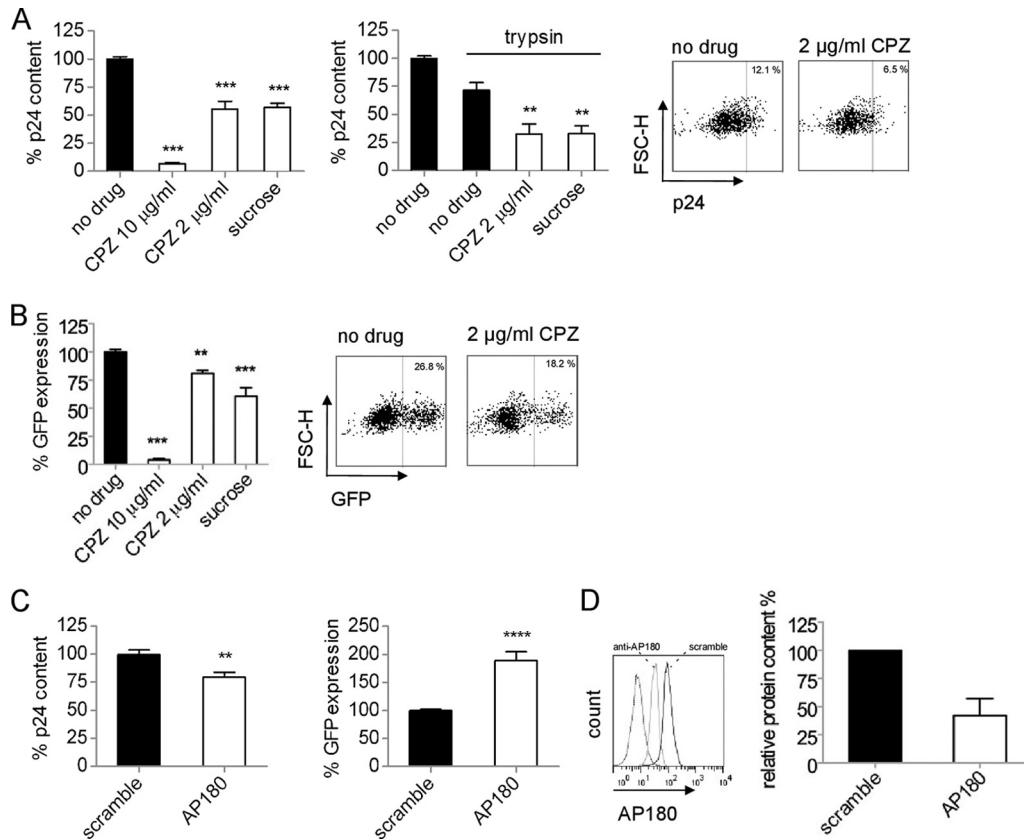
FIG 3 Association between endocytosis, virus transfer into target cells, and productive infection during cell-to-cell transmission. (A) Relative p24 content of target cells during cell-to-cell transmission between PM1 cells using X4-tropic NL4-3-derived virus. Endocytosis was antagonized by pretreatment of target cells with chlorpromazine (CPZ) or hypertonic sucrose. In some instances cells were treated with trypsin prior to analysis. Representative flow cytometry data are shown. (B) Relative reporter virus GFP expression of target cells during cell-to-cell transmission. Endocytosis was antagonized by pretreatment of target cells with chlorpromazine (CPZ) or hypertonic sucrose. Representative flow cytometry results are shown. (C) Relative p24 content or reporter virus GFP expression of target cells during cell-to-cell transmission in studies in which levels of the clathrin accessory protein AP180 were depleted in target cells via the expression of an shRNA directed against it. Representative flow cytometry results are shown. (D) Confirmation of AP180 knockdown in PM1 cells via shRNA expression. shRNAs were expressed via transduction and IPTG induction. Intracellular staining by flow cytometry confirmed knockdown; a representative histogram and mean data are shown. All data are means ± SEM ($n \geq 3$); statistically significant results relative to controls (black columns) are indicated.

surface and the site of clathrin-coated pit formation (49). Chlorpromazine-treated cells were incubated with HIV-infected donor cells. We found that 10 μg/ml and 2 μg/ml of chlorpromazine produced a 93% and 46% reduction, respectively, in target cell p24 content (Fig. 3A). Trypsin treatment of these cultures prior to p24 staining yielded a similar reduction in target cell p24 content compared to that in trypsin-treated controls. This reduction in p24 uptake in target cells was also related to productive infection, yielding a 93% or 19% reduction in target cell GFP expression, detectable at 24 h after 10 μg/ml or 2 μg/ml chlorpromazine pretreatment and washout, respectively (Fig. 3B), in the absence of toxic effects (Fig. 2F).

Treatment of cells with hypertonic sucrose medium (0.45 M) is thought to reduce clathrin-coated pit formation and subsequently inhibit endocytosis (50), and so we pretreated labeled PM1 target cells with sucrose for 45 min prior to washout and coculture with infected cells. This reduced the transfer of virus from infected donor cells, resulting in an almost 2-fold reduction in target cell p24 content, both following and in the absence of trypsin treatment (Fig. 3A), as well as a 39% reduced rate of infection as measured by virus GFP expression in target cells (Fig. 3B).

Though chlorpromazine and sucrose are historically considered useful inhibitors of clathrin-mediated endocytosis, certain analyses suggest that they may exert a more global effect on endosomal uptake of ligands (48, 51) while some investigators argue chlorpromazine may still be a useful indicator of this process (28, 49). However, further attempts to disrupt clathrin-mediated endocytosis in a more specific manner using the small-molecule inhibitor Pitstop 2 were unsuccessful (29) as we were unable to antagonize transferrin uptake in either PM1 or Jurkat cells across a range of concentrations (data not shown).

Therefore, to better define the role of clathrin-mediated endocytosis, we transduced PM1 cells with a lentivirus that expresses either control or anti-AP180 shRNAs upon induction as AP180 is an important accessory protein in clathrin-mediated endocytosis that binds both membrane lipids and clathrin (48). We observed a 60% reduction in total cellular AP180 content (Fig. 3D), and we therefore induced shRNA expression for 72 h prior to and during infected cell coculture. This led to a modest but significant 20% reduction in PM1 cell p24 uptake during cell-to-cell transmission (Fig. 3C), implying some role for clathrin-mediated endocytosis in viral uptake. Yet, surprisingly, expression of this shRNA ulti-
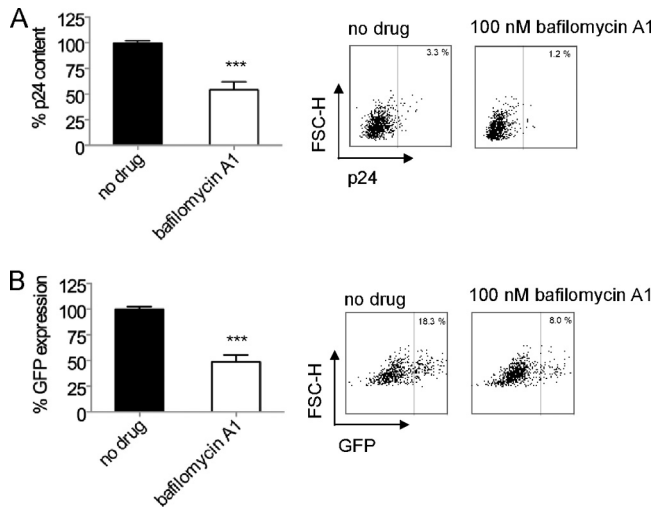
FIG 4 Endosomal acidification in target cells during cell-to-cell transmission. (A) Relative p24 content of target cells during cell-to-cell transmission between PM1 cells using X4-tropic NL4-3-derived virus. Endosomal acidification and turnover were antagonized by the pretreatment of target cells with bafilomycin A. Representative flow cytometry data are shown. (B) Relative reporter virus GFP expression of target cells during cell-to-cell transmission. Endosomal acidification and turnover were antagonized by pretreatment of target cells with bafilomycin A. Representative flow cytometry results are shown. All data are means ± SEM ($n \geq 3$); statistically significant results relative to controls (black columns) are indicated.
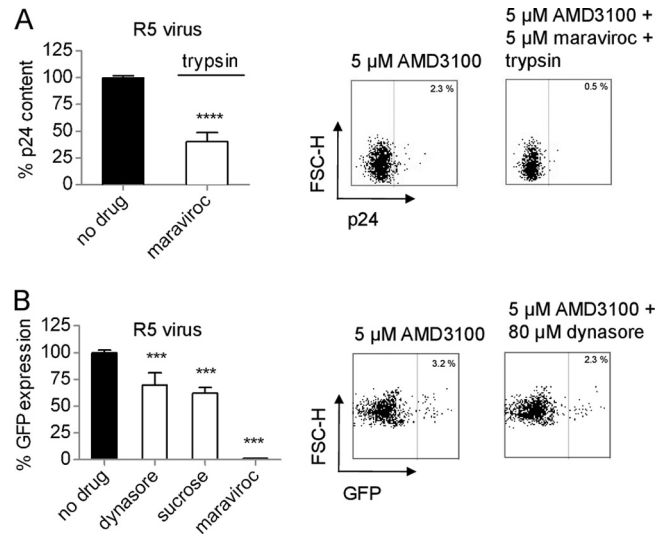

FIG 5 Productive infection via dynamin-dependent endocytosis using CCR5-tropic HIV-1. (A) Relative p24 content of target cells during cell-to-cell transmission between PM1 cells using R5-tropic NL4-3-derived virus. Coreceptor binding was antagonized by treatment of cells with the CCR5 antagonist maraviroc or the CXCR4 antagonist AMD3100. Some cells were treated with trypsin prior to analysis. Representative flow cytometry data are shown. (B) Relative reporter virus GFP expression of target cells in which coreceptor binding was antagonized by treatment of cells with the CCR5 antagonist maraviroc or the CXCR4 antagonist AMD3100. Representative flow cytometry results are shown. All data are means ± SEM ($n \geq 3$); statistically significant results relative to controls (black columns) are indicated.

mately led to an ~2-fold increase in the number of infected target cells as measured by GFP expression (Fig. 3C). Taken together, these data demonstrate that endosomal uptake of HIV-1 contributes to productive infection, adding to our antiviral and dynamin analysis, but they cannot definitively implicate clathrin-mediated endocytosis in this role.

Disrupting endosomal acidification in target cells diminishes HIV-1 uptake during cell-to-cell transmission. The treatment of PM1 cells with shRNA targeted to the clathrin accessory protein AP180 ultimately led to an enhanced rate of infection but in a manner that could not be linked to increased uptake. We therefore wished to investigate if the use of endosomal acidification inhibitors might also augment rates of productive infection, as had been noted in prior studies. Such data have been interpreted in two ways: (i) delaying the steady-state turnover of endocytic vesicles allows HIV-1 that has entered them to achieve productive entry before lysosomal degradation of virus from within a typically nonproductive pathway has occurred (52, 53), or (ii) inhibiting endosomal acidification diverts virus out of a nonproductive endocytic pathway toward a productive cell-surface entry pathway (23).

To determine if parallels could exist with our own AP180 RNAi data, we performed cell-to-cell transmissions using PM1 cells that had been pretreated for 45 min with bafilomycin A1, an endosomal acidification inhibitor. Unlike the situation for cell-free infection, we noted that preventing endosomal acidification led to an ~2-fold reduction in the uptake of viral p24 into target cells and that this translated into an ~2-fold reduction in the infection rate of these cells (Fig. 4). Thus, the antiviral effect associated with inhibition of endosomal acidification with bafilomycin A1 was linked to a virus uptake defect associated with the drug. This is also consistent with other studies that showed that inhibiting endo-

somal acidification leads to a decrease in the steady state of endocytic vesicle turnover (53, 54). Thus, these findings place HIV-1 within a productive entry route associated with target cell endocytic vesicle uptake, yet these data are not consistent with results from cell-free infections showing that disrupting endosomal acidification can enhance infection (23, 52, 53), suggesting a fundamental difference between endosomal uptake of HIV-1 during cell-free and cell-associated infection.

Productive entry of CCR5-tropic virus via target cell endocytosis. Previous experiments were carried out with an X4-tropic virus. Since CCR5 is the major coreceptor for HIV-1 on both CD4$^+$ T cells and macrophages, we sought to confirm our findings using R5-tropic virus in the PM1 cell line which expresses CCR5 in addition to CXCR4 (55). We infected PM1 donor cells to a maximal rate of 5 to 10% GFP positivity with an R5-tropic reporter virus, and cocultured them with PM1 target cells treated with the CCR5 antagonist maraviroc both before and during coculture transmissions. This treatment partially reduced the rate of p24 detectable in trypsin-resistant compartments in target cells (60%) yet completely blocked GFP expression in target cells (Fig. 5A and B), implying that a significant proportion of coreceptor binding occurs inside target cells for R5-tropic virus, as seen with X4-tropic virus (Fig. 1B).

We next used R5-tropic virus in PM1 cell-to-cell transmission experiments in which we antagonized cellular dynamin function by pretreating cells with dynasore. As with X4-tropic virus, this led to a modest but reproducible reduction in the rate of target cell infection (30%) at 24 h after pretreatment and drug washout (Fig. 5B). Equally, when endocytosis was inhibited in target cells via hypertonic sucrose pretreatment, productive infection of R5-

tropic virus was again inhibited, yielding a 38% reduction in the rate of infected target cells (Fig. 5B).

Notably, we never observed syncytia during infection of PM1 target cells with R5-tropic virus, even at 72 h postinfection. Given that the same patterns of results were seen with X4-tropic and R5-tropic virus, this further confirms that the previous results with X4-tropic virus did not arise from cell-cell fusions.

Collectively, these data show that dynamin-dependent and clathrin-mediated endocytosis is a viable and productive entry route for R5-tropic as well as X4-tropic virus and that coreceptor binding during this process may occur from within trypsin-resistant compartments in the target cell.

Productive cell-to-cell infection of multiple CD4$^+$ T-cell lines via endocytosis. Having established that productive infection of PM1 cells can occur via endocytosis in a dynamin- and clathrin-dependent manner, we next asked if these findings were applicable to other CD4$^+$ T-cell lines and allogeneic transmission pairs (i.e., transmission between genetically distinct cells of the same species). Therefore, we performed experiments using transmissions from infected Jurkat cells (maximally 5 to 10% GFP positive) to Jurkat cells pretreated with the dynamin antagonist dynasore and found that this resulted in a 24% decrease in target cell viral uptake (Fig. 6A). Similar findings were observed in RNAi assays as induction of an anti-dynamin-2 shRNA in Jurkat target cells (Fig. 6B) yielded a 61% reduction in viral p24 uptake and a 41% reduction in viral GFP expression in target cells (Fig. 6C). As with PM1 cells, these results confirm that dynamin-mediated uptake of virus between Jurkat cells can lead to productive entry and infection.

We next analyzed the role of endocytosis during cell-to-cell transmission between Jurkat cells. Hypertonic sucrose pretreatment of Jurkat target cells reduced p24 uptake by 39% (Fig. 6A). As with PM1 cells, we transduced Jurkat cells to express an shRNA targeted to AP180 shRNA upon induction (Fig. 6B). The results indicate a 30% reduction in Jurkat target cell p24 uptake, but, as with PM1 cells, we observed an enhanced rate of infection (<2-fold) (Fig. 6C).

To study if the endocytosis phenotype was also operative in allogeneic cell-to-cell transmissions, we performed studies in which HIV was transferred from PM1 cells to Jurkat cells. Endocytosis was inhibited with either hypertonic sucrose or by shRNAs. The data indicate that PM1-to-Jurkat cell-to-cell transmissions occurred in a dynamin-dependent manner as anti-dynamin-2 shRNA reduced p24 uptake in Jurkat target cells by 40%. This treatment also led to reductions in rates of viral GFP expression in Jurkat target cells (43%), again indicating that the dynamin-dependent route was important for HIV-1 infection (Fig. 6F). However, blockage of clathrin-mediated endocytosis by hypertonic sucrose pretreatment neither reduced nor enhanced target cell uptake of viral p24 nor affected subsequent viral GFP expression (Fig. 6F). Equally, depletion of AP180 in target cells yielded similar data as expression of shRNAs against AP180 had no significant effect on viral uptake and produced only a very modest increase in rates of target cell infection (12%) (Fig. 6F).

These data led us to investigate whether there was deficit in clathrin-mediated endocytosis in the Jurkat cells used in these experiments, and so we assayed their ability to take up transferrin, which is commonly incorporated into cells via clathrin-mediated endocytosis. However, we found that this pathway was intact and could be readily antagonized by hypertonic sucrose treatments

(data not shown). Therefore, although productive viral entry during cell-to-cell transmission between PM1 cells and Jurkat cells is dynamin dependent, this process appears to be independent of the canonical route of clathrin-mediated endocytosis and cannot be attributed to caveolar endocytosis.

To investigate if allogeneic HIV-1 transmissions were always dysfunctional in the clathrin-associated antagonist-sensitive route, we performed cell-to-cell transmissions from PM1 donor cells to SupT1 CD4$^+$ T cells and pretreated the latter with hypertonic sucrose. Virus transfer and transmission were found to be reduced, as shown by a 45% reduction in p24 uptake and a 26% reduction in viral GFP expression in SupT1 target cells (Fig. 6G). Therefore, productive transmission to SupT1 cells from PM1 cells involves a clathrin-mediated endocytic entry route, unlike transmissions from PM1 to Jurkat cells.

Productive infection of primary CD4$^+$ T cells via endocytosis. Finally, we wished to confirm the role of the clathrin-mediated endocytic entry route in primary activated CD4$^+$ T cells, the predominant target of HIV-1 *in vivo*. We first purified primary CD4$^+$ T cells from donor peripheral blood mononuclear cells (PBMCs) by negative selection and activated them via PHA stimulation for 72 h. We then performed a cell-to-cell transmission assay with PM1 cells acting as donor cells and cell tracker-stained, activated primary CD4$^+$ T cells as targets. To inhibit endocytosis, primary CD4$^+$ T cells were pretreated with hypertonic sucrose prior to coculture. As with the other transmissions, we found that hypertonic sucrose treatment of primary CD4$^+$ T cells significantly reduced the rate of target cell infection, i.e., ~2-fold, relative to untreated controls.

To exclude artifacts arising from the use of a cell line as the donor cell and because our prior analysis suggested that allogeneic transmissions may be dysfunctional for the clathrin-associated antagonist endocytosis uptake phenotype, we performed a series of autologous transmissions between purified activated CD4$^+$ T cells isolated from four individual donors. Cells were first activated by anti-CD3/anti-CD28 stimulation and then infected with X4-tropic GFP reporter virus before use in cell-to-cell transmission assays using stained target cells isolated from the same donor. Endocytosis was inhibited in target cells using both hypertonic sucrose treatment and 2 μg/ml chlorpromazine. As with all prior analyses, disruption of endocytosis in target cells reduced the rate of infection, confirming that, as with cell lines, productive infection of HIV-1 via endocytosis is apparent in cell-to-cell transmission among primary activated CD4$^+$ T cells (Fig. 7B).

DISCUSSION

Using genetic and pharmacologic approaches to measure both viral uptake and productive infection, we have now shown that HIV-1 utilizes a dynamin-dependent endocytic entry pathway to productively infect CD4$^+$ T cells during cell-to-cell transmission. This was shown in a number of cell lines and is a finding also demonstrated here in primary CD4$^+$ T cells. Given that all homologous transmissions and primary cell analyses converged on the same phenotype, we propose that productive endocytosis during cell-to-cell transmission occurs *in vivo*. By probing the viral entry cascade with HIV-1 entry inhibitors, we have shown that entry into trypsin-resistant compartments in target cells requires gp120-CD4 interactions, while we also show that a significant proportion of virus-coreceptor interactions, and all virus-cell fusion events, can occur from within such compartments, supporting prior findings (24, 36). These data were found for both X4-tropic
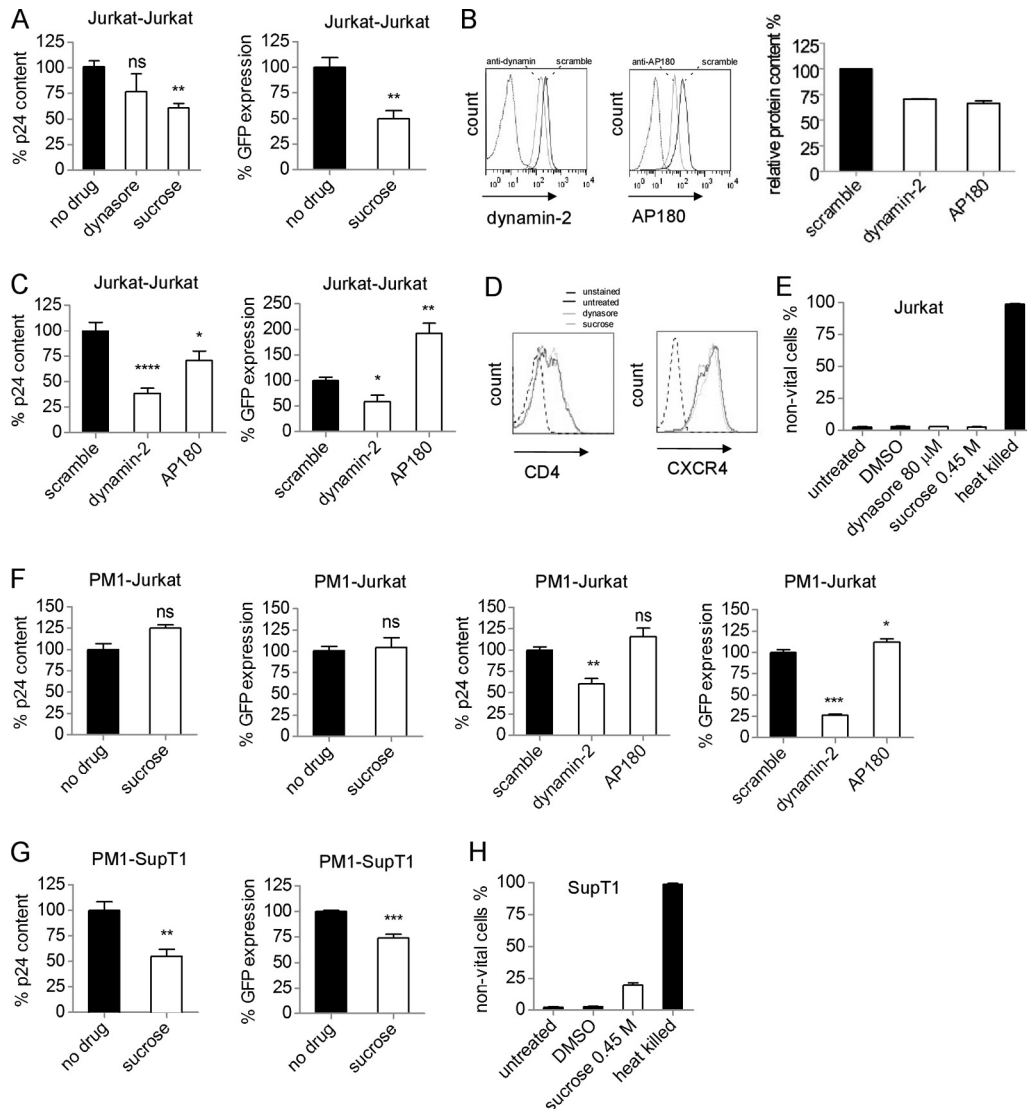
FIG 6 Productive infection via dynamin-dependent endocytosis in multiple CD4$^+$ T-cell lines. (A) Relative p24 content and reporter virus GFP expression of target cells during cell-to-cell transmission between Jurkat cells using X4-tropic NL4-3-derived virus. Dynamin was antagonized with dynasore while endocytosis was inhibited by hypertonic sucrose treatment. (B) Confirmation of dynamin-2 and AP180 knockdown in Jurkat cells via shRNA expression. shRNAs were expressed via transduction and IPTG induction. Intracellular staining by flow cytometry confirmed knockdown; representative histograms and mean data are shown. (C) Relative p24 content and reporter virus GFP expression of target cells during cell-to-cell transmission between Jurkat cells in which dynamin-2 or AP180 was depleted via shRNA expression. (D) Expression of cell surface CD4 or CXCR4 on Jurkat cells 2 h following dynasore or hypertonic sucrose treatment. Representative histograms are shown. (E) Cellular viability of Jurkat cells following treatment with endocytosis inhibitors relative to heat-killed cells. (F) Relative p24 content and reporter virus GFP expression of target cells during cell-to-cell transmission from PM1 cells to Jurkat cells using X4-tropic NL4-3-derived virus. Dynamin-2 was antagonized by shRNA expression, while endocytosis was inhibited by hypertonic sucrose treatment or expression of shRNAs against the clathrin accessory protein AP180. (G) Relative p24 content and reporter virus GFP expression of target cells during cell-to-cell transmission from PM1 cells to SupT1 cells using X4-tropic NL4-3-derived virus. Endocytosis was inhibited by hypertonic sucrose treatment. (H) Cellular viability of SupT1 cells following treatment with endocytosis inhibitors relative to heat-killed cells. All data are means ± SEM ($n \geq 3$); statistically significant results relative to controls (black columns) are indicated.

and R5-tropic HIV-1, implying no fundamental difference in their endosomal entry modes. Taken together, our findings on HIV-1 entry inhibition and on inhibition of cellular endocytosis suggest a mode of HIV-1 entry from within cellular endocytic vesicles, allowing HIV-1 to enter the cell via dynamin-dependent endocytic processes. These data are in agreement with a recent study in which viral protease-mediated maturation of HIV-1 within cellular endosomes was shown to drive virus-cell membrane fusion events within endosomes during cell-to-cell trans-

mission (24). Further, our data build on the findings of other studies that describe viruses in endosome-like structures in target cells engaged in virological synapses; these are likely to be engaged in productive infection via dynamin-dependent endocytosis (21, 22). Finally, our data are consistent with findings of cell-free entry of HIV-1, i.e., entry of virus into CD4$^+$ T cells in a dynamin-dependent manner via cellular fusion in endosomes (28).

Conceivably, the reductions in target cell p24 uptake and GFP expression that we observed might be due to a reduction in the
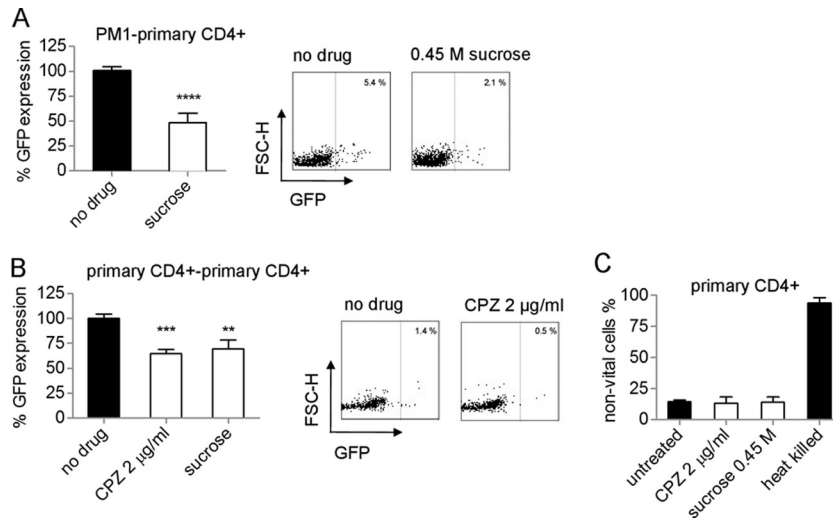
FIG 7 Productive infection via endocytosis in primary CD4+ T cells. (A) Relative reporter virus GFP expression of target cells during cell-to-cell transmission from PM1 cells to PHA-activated primary CD4+ T cells using X4-tropic NL4-3-derived virus. Endocytosis was inhibited by hypertonic sucrose treatment. Representative flow cytometry results are shown. (B) Relative reporter virus GFP expression of target cells during autologous cell-to-cell transmissions between anti-CD3/anti-CD28-activated primary CD4+ T cells using X4-tropic NL4-3 derived virus. Endocytosis was inhibited by hypertonic sucrose treatment or 2 μg/ml chlorpromazine (CPZ). Mean results from four individual donors assayed in triplicate are presented. Representative flow cytometry results are shown. (C) Cellular viability of primary activated CD4+ T cells following treatment with endocytosis inhibitors relative to heat killed cells. All data are means ± SEM.

ability of endocytosis-inhibited cells to bring about interactions with infected donor cells. However, the concept of endosomal uptake is also supported by our antiviral analysis (Fig. 1), confirming that our results are not due to artifacts associated with disruption of endocytosis. We found no disruption of CD4 or coreceptor levels in target cells after endocytosis treatments, which were also shown to be nontoxic (Fig. 2, 6, and 7). Nor did we find a decrease in the rate of cells measured as doublets (or larger) via pulse width, irrespective of the treatments used to disrupt endocytosis, suggesting that these treatments did not inhibit the formation of cell-cell contacts and so should not inhibit the likelihood of virological synapse formation (data not shown).

In this study, we made use of a number of small molecular inhibitors of endocytosis, a common approach in the analysis of cellular trafficking or cytoskeletal regulation. If toxicity and off-target effects are controlled for, such analysis can be revealing, especially if unrelated compounds and supporting genetic analyses converge on the same phenotype as seen here (48, 49, 51). This is an approach that has already been successfully employed to study cell-to-cell transmission or endocytosis of HIV-1 (14, 28). Although the phenotypes we report here are generally modest (~2 to 5-fold), we suspect that they are an underestimate due to pre-treatment and washout of endocytosis inhibitors prior to analysis or due to incomplete shRNA-mediated suppression of protein expression. Thus, our data augment the body surrounding endosomal entry of HIV-1 by confirming that coreceptor binding and virus-cell membrane fusion can occur from within target cells (24, 36) and show that dynamin-dependent endocytic pathways can lead to productive HIV-1 cell-to-cell transmission, a process that has thus far been ill defined.

One interpretation of our data may be that they indicate dynamin-dependent entry at the cell surface. Yet the use of antiviral drugs that block HIV-1 entry in our study and others suggests that most entry processes downstream of CD4 binding occur from within trypsin-resistant compartments, compartments that we

along with other investigators interpret to be endocytic vesicles (24, 36). Recent data also suggest a role for dynamin in regulating cellular membrane fusion pores (56), leading to proposals that dynamin may also regulate viral fusion pores, too (57). Indeed, during cell-free entry of HIV, dynamin has been shown to regulate viral fusion from within endosomes (28) though it appears unable to mediate complete viral fusion at the cell surface (26). Nor do our data regarding the pharmacologic inhibition of endocytosis support the notion of dynamin-dependent cell surface entry (Fig. 3 and 4). Further, our antiviral analysis suggests that membrane fusion occurs from within endosomes (Fig. 1). Thus, we consider dynamin-dependent endocytosis to be the most valid conclusion from our data. The two predominant dynamin-dependent endocytosis uptake routes in cells are caveolar endocytosis and clathrin-mediated endocytosis. Caveolar uptake of HIV-1 in lymphocytes is unlikely, given their paucity of caveolin-1 expression and apparent lack of caveolae (44–47). Although one study did note caveolin-1 expression in primary CD4+ T cells engaged in virological synapses, viral p24 was not found to colocalize with caveolin-1 (22). Although we were not able to definitively implicate clathrin-mediated endocytosis, due to our concerns regarding the absolute specificity of sucrose and chlorpromazine, our AP180 depletion data suggest that this route does affect viral uptake, at least in part. However, the enhanced infection rates seen with AP180 depletion clouds this interpretation. Nonetheless, we consider clathrin-mediated endocytosis to be the most likely uptake route, a conclusion that is in agreement with prior studies of cell-free HIV-1 infection (25, 58).

It is unclear why AP180 depletion should decrease viral uptake but enhance infection. Such findings are reminiscent of those surrounding the Lv2 restriction phenotype of HIV-2, in which depletion of dynamin-2 or the clathrin adaptor AP-2 also led to enhanced infection (58, 59). The Lv2 studies suggested that diverting virus out of endocytic pathways in which restriction is found can rescue infection. Such a hypothesis may be tenable for our data,

given descriptions of the interferon-induced transmembrane family of proteins (IFITMs) as being associated with endocytic pathways and modestly affecting HIV-1 replication (60, 61). An alternative possibility is that AP180 depletion may somehow render the cell more amenable to viral infection, perhaps due to AP180-lipid interactions (48), though this remains speculative and was not seen with dynamin, which has significant membrane shaping properties (38). A final possibility is that endosomal uptake is more likely during cell-to-cell transmission due to the virus being caught up in ongoing endocytic processes at the virological synapse. From the endocytic vesicles, the virus might attain low-efficiency entry which might, in part, be overcome by the high multiplicity of infection associated with cell-to-cell transmission (62). Therefore, depleting AP180 may divert virus entry into a cell surface mode that is intrinsically more efficient but typically less apparent at the virological synapse unless AP180 is depleted. Such a hypothesis requires confirmation but is in agreement with a compensatory link between cell surface and endosomal entry during cell-free HIV-1 transmission (23). However, our data cannot rule out indirect effects of AP180 depletion on endocytosis. Yet we did see that the AP180- and sucrose-associated phenotypes, present in autologous transmissions between PM1 cells or between Jurkat cells, were both unapparent with these treatments in allogeneic transmissions between PM1 cells and Jurkat cells. This suggests that both treatments do target the same virus uptake endocytic pathway that became similarly defective during allogeneic transmissions.

These data do provide clearer evidence of entry pathway flexibility as allogeneic cell-to-cell transmissions of HIV-1 from PM1 cells to Jurkat cells were still dynamin dependent, but antagonism of AP180 with shRNAs or disruption of endocytosis via hypertonic sucrose treatment had no effect on either viral uptake or transmission. Interestingly, no enhancement of infection with AP180 depletion was seen either. Why transmission from PM1 to Jurkat cells should not allow virus to enter via clathrin-mediated endocytosis is unclear, but the data imply that *in vivo* phenotypes might not always be recapitulated in allogeneic cell culture assays of cell-to-cell transmission. This point is of some concern, given that a significant proportion of published data on cell-to-cell transmission of HIV-1 does involve such allogeneic transmissions. However, cell-to-cell transmission of HIV-1 between CD4$^+$ T cells in lymphoid tissue should only occur between autologous cells; our autologous transmission data are consistent with the notion that transmission via endocytosis occurs *in vivo*.

We are not alone in suggesting that HIV-1 entry during cell-to-cell transmission might be flexible, and others have proposed that this could account for variable observations regarding productive endocytic entry of HIV-1 or in cell-to-cell transmission (63–65), a viewpoint that might argue against excessive reliance on single infection models. Given the range of infection models that have been reported in the literature, future studies might benefit from greater emphasis on primary cell and genetic analyses. Nonetheless, it is already apparent that during cell-free infection HIV-1 can engage in both cell surface fusion and endocytic entry in CD4$^+$ T cells, with different cell lines and viruses varying in their capacities to support both entry modes (23, 25–27, 29). HIV-1 has also been suggested to use macropinocytosis or noncanonical dynamin-mediated endocytosis to enter macrophages (39, 63, 66), with data showing that endocytic entry into macrophages depends on the cytokine environment, differentiation and

activation status, and overall function of the endosomal-lysosomal pathway (67). Further, HIV-1 can use caveolar endocytosis to enter plasmacytoid dendritic cells (40). Thus, the evidence of cell-free endosomal entry and pathway flexibility of HIV-1 is rapidly accumulating. When paired with studies suggesting endosomal entry during cell-to-cell transmission of HIV-1 (21, 22, 24) and the data presented in the manuscript that identify a role for dynamin-dependent endocytosis in productive infection, a picture emerges of a virus with considerable flexibility to use various entry modes.

Several studies have not documented viral uptake by endocytosis during cell-to-cell transmission of HIV-1 between T cells (5, 6, 20). As we have noted, the mix of experimental approaches used makes it difficult to reconcile all differences. We have described cell line-associated transmission deficits during allogeneic transmissions (Fig. 6), and a recent study has also now found evidence for cell line-based differences during cell-to-cell HIV-1 transmission (65). It now remains to better define the circumstances that dictate the likelihood of particular entry pathways being used by either cell-free or cell-associated virus and to determine whether differences in pathway utilization can explain the divergent data in the literature (64).

Overall, we have shown that the cellular membrane scission protein dynamin-2 is predominantly involved in mediating the productive uptake of virus containing endocytic vesicles, resulting in productive HIV-1 entry via the virological synapse. Defining the remaining mechanisms underlying productive infection in target cells during cell-to-cell transmission will be important. There may still be some useful parallels between mechanisms in found in immunological synapses despite the admittedly incomplete analogy with the virological synapse (68). For example, given that HIV-1 can egress from infected CD4$^+$ T cells via the secretory machinery used in CD4$^+$ T-cell immunological synapses (19), there may be a role for coupled endocytosis and exocytosis (30) in the HIV-1 virological synapse. Equally, intercellular protein transfer processes such as trogocytosis and transendocytosis that are thought to be active in immunological synapses may also be found to be important for HIV-1 transmission (69). More widely, an improved understanding of the role of target cell endocytosis may help to resolve issues relating to the capacity of virus to evade neutralizing antibodies during cell-to-cell transmission due to the presence of HIV-1 within immunologically privileged endocytic compartments (1, 20, 24, 65, 70–72). Hopefully, better understanding of cell-to-cell transmission will then lead to new or improved therapeutic approaches for inhibiting HIV-1 infection.

REFERENCES

1. **Chen P, Hübner W, Spinelli MA, Chen BK.** 2007. Predominant mode of human immunodeficiency virus transfer between T cells is mediated by sustained Env-dependent neutralization-resistant virological synapses. J. Virol. **81**:12582–12595.

2. **Murooka TT, Deruaz M, Marangoni F, Vrbanac VD, Seung E, von Andrian UH, Tager AM, Luster AD, Mempel TR.** 2012. HIV-infected T cells are migratory vehicles for viral dissemination. Nature **490**:283–287.

3. **Grakoui A, Bromley SK, Sumen C, Davis MM, Shaw AS, Allen PM, Dustin ML.** 1999. The immunological synapse: a molecular machine controlling T cell activation. Science **285**:221–227.

4. **Igakura T, Stinchcombe JC, Goon PK, Taylor GP, Weber JN, Griffiths GM, Tanaka Y, Osame M, Bangham CR.** 2003. Spread of HTLV-I between lymphocytes by virus-induced polarization of the cytoskeleton. Science **299**:1713–1716.

5. **Jolly C, Kashefi K, Hollinshead M, Sattentau QJ.** 2004. HIV-1 cell to cell transfer across an Env-induced, actin-dependent synapse. J. Exp. Med. **199**:283–293.

6. **Rudnicka D, Feldmann J, Porrot F, Wietgrefe S, Guadagnini S, Prévost MC, Estaquier J, Haase AT, Sol-Foulon N, Schwartz O.** 2009. Simultaneous cell-to-cell transmission of human immunodeficiency virus to multiple targets through polysynapses. J. Virol. **83**:6234–6246.

7. **Groot F, Welsch S, Sattentau QJ.** 2008. Efficient HIV-1 transmission from macrophages to T cells across transient virological synapses. Blood **111**:4660–4663.

8. **Sowinski S, Jolly C, Berninghausen O, Purbhoo MA, Chauveau A, Köhler K, Oddos S, Eissmann P, Brodsky FM, Hopkins C, Onfelt B, Sattentau Q, Davis DM.** 2008. Membrane nanotubes physically connect T cells over long distances presenting a novel route for HIV-1 transmission. Nat. Cell Biol. **10**:211–219.

9. **Lehmann MJ, Sherer NM, Marks CB, Pypaert M, Mothes W.** 2005. Actin- and myosin-driven movement of viruses along filopodia precedes their entry into cells. J. Cell Biol. **170**:317–325.

10. **Sherer NM, Lehmann MJ, Jimenez-Soto LF, Horensavitz C, Pypaert M, Mothes W.** 2007. Retroviruses can establish filopodial bridges for efficient cell-to-cell transmission. Nat. Cell Biol. **9**:310–315.

11. **Geijtenbeek TB, Kwon DS, Torensma R, van Vliet SJ, van Duijnhoven GC, Middel J, Cornelissen IL, Nottet HS, KewalRamani VN, Littman DR, Figdor CG, van Kooyk Y.** 2000. DC-SIGN, a dendritic cell-specific HIV-1-binding protein that enhances trans-infection of T cells. Cell **100**:587–597.

12. **Dale BM, Alvarez RA, Chen BK.** 2013. Mechanisms of enhanced HIV spread through T-cell virological synapses. Immunol. Rev. **251**:113–124.

13. **Sattentau QJ.** 2010. Cell-to-cell spread of retroviruses. Viruses **2**:1306–1321.

14. **Jolly C, Mitar I, Sattentau QJ.** 2007. Requirement for an intact T-cell actin and tubulin cytoskeleton for efficient assembly and spread of human immunodeficiency virus type 1. J. Virol. **81**:5547–5560.

15. **Jolly C, Sattentau QJ.** 2005. Human immunodeficiency virus type 1 virological synapse formation in T cells requires lipid raft integrity. J. Virol. **79**:12088–12094.

16. **Jolly C, Mitar I, Sattentau QJ.** 2007. Adhesion molecule interactions facilitate human immunodeficiency virus type 1-induced virological synapse formation between T cells. J. Virol. **81**:13916–13921.

17. **Jolly C, Sattentau QJ.** 2007. Human immunodeficiency virus type 1 assembly, budding, and cell-cell spread in T cells take place in tetraspanin-enriched plasma membrane domains. J. Virol. **81**:7873–7884.

18. **Sol-Foulon N, Sourisseau M, Porrot F, Thoulouze MI, Trouillet C, Nobile C, Blanchet F, di Bartolo V, Noraz N, Taylor N, Alcover A, Hivroz C, Schwartz O.** 2007. ZAP-70 kinase regulates HIV cell-to-cell spread and virological synapse formation. EMBO J. **26**:516–526.

19. **Jolly C, Welsch S, Michor S, Sattentau QJ.** 2011. The regulated secretory pathway in CD4$^+$ T cells contributes to human immunodeficiency virus type-1 cell-to-cell spread at the virological synapse. PLoS Pathog. **7**:e1002226. doi:10.1371/journal.ppat.1002226.

20. **Martin N, Welsch S, Jolly C, Briggs J, Vaux D, Sattentau Q.** 2010. Virological synapse-mediated spread of human immunodeficiency virus type 1 between T cells is sensitive to entry inhibition. J. Virol. **84**:3516–3527.

21. **Hübner W, McNerney GP, Chen P, Dale BM, Gordon RE, Chuang FY, Li XD, Asmuth DM, Huser T, Chen BK.** 2009. Quantitative 3D video microscopy of HIV transfer across T cell virological synapses. Science **323**:1743–1747.

22. **Bosch B, Grigorov B, Senserrich J, Clotet B, Darlix JL, Muriaux D, Este JA.** 2008. A clathrin-dynamin-dependent endocytic pathway for the uptake of HIV-1 by direct T cell-T cell transmission. Antiviral Res. **80**:185–193.

23. **Schaeffer E, Soros VB, Greene WC.** 2004. Compensatory link between fusion and endocytosis of human immunodeficiency virus type 1 in human CD4 T lymphocytes. J. Virol. **78**:1375–1383.

24. **Dale BM, McNerney GP, Thompson DL, Hubner W, de Los Reyes K, Chuang FY, Huser T, Chen BK.** 2011. Cell-to-cell transfer of HIV-1 via virological synapses leads to endosomal virion maturation that activates viral membrane fusion. Cell Host Microbe **10**:551–562.

25. **Daecke J, Fackler OT, Dittmar MT, Kräusslich HG.** 2005. Involvement of clathrin-mediated endocytosis in human immunodeficiency virus type 1 entry. J. Virol. **79**:1581–1594.

26. **de la Vega M, Marin M, Kondo N, Miyauchi K, Kim Y, Epand RF, Epand RM, Melikyan GB.** 2011. Inhibition of HIV-1 endocytosis allows lipid mixing at the plasma membrane, but not complete fusion. Retrovirology **8**:99. doi:10.1186/1742-4690-8-99.

27. **Fackler OT, Peterlin BM.** 2000. Endocytic entry of HIV-1. Curr. Biol. **10**:1005–1008.

28. **Miyauchi K, Kim Y, Latinovic O, Morozov V, Melikyan GB.** 2009. HIV enters cells via endocytosis and dynamin-dependent fusion with endosomes. Cell **137**:433–444.

29. **von Kleist L, Stahlschmidt W, Bulut H, Gromova K, Puchkov D, Robertson MJ, Macgregor KA, Tomlin N, Pechstein A, Chau N, Chircop M, Sakoff J, von Kries JP, Saenger W, Kräusslich HG, Shupliakov O, Robinson PJ, McCluskey A, Haucke V.** 2011. Role of the clathrin terminal domain in regulating coated pit dynamics revealed by small molecule inhibition. Cell **146**:471–484.

30. **Griffiths GM, Tsun A, Stinchcombe JC.** 2010. The immunological synapse: a focal point for endocytosis and exocytosis. J. Cell Biol. **189**:399–406.

31. **Schindler M, Münch J, Kirchhoff F.** 2005. Human immunodeficiency virus type 1 inhibits DNA damage-triggered apoptosis by a Nef-independent mechanism. J. Virol. **79**:5489–5498.

32. **Kuhl BD, Sloan RD, Donahue DA, Bar-Magen T, Liang C, Wainberg MA.** 2010. Tetherin restricts direct cell-to-cell infection of HIV-1. Retrovirology **7**:115. doi:10.1186/1742-4690-7-115.

33. **Maréchal V, Clavel F, Heard JM, Schwartz O.** 1998. Cytosolic Gag p24 as an index of productive entry of human immunodeficiency virus type 1. J. Virol. **72**:2208–2212.

34. **Münch J, Rücker E, Ständker L, Adermann K, Goffinet C, Schindler M, Wildum S, Chinnadurai R, Rajan D, Specht A, Giménez-Gallego G, Sánchez PC, Fowler DM, Koulov A, Kelly JW, Mothes W, Grivel JC, Margolis L, Keppler OT, Forssmann WG, Kirchhoff F.** 2007. Semen-derived amyloid fibrils drastically enhance HIV infection. Cell **131**:1059–1071.

35. **Schindler M, Münch J, Kutsch O, Li H, Santiago M, Bibollet-Ruche F, Müller-Trutwin M, Novembre F, Peeters M, Courgnaud V, Bailes E, Roques P, Sodora D, Silvestri G, Sharp P, Hahn B, Kirchhoff F.** 2006. Nef-mediated suppression of T cell activation was lost in a lentiviral lineage that gave rise to HIV-1. Cell **125**:1055–1067.

36. **Blanco J, Bosch B, Fernández-Figueras MT, Barretina J, Clotet B, Esté JA.** 2004. High level of coreceptor-independent HIV transfer induced by contacts between primary CD4 T cells. J. Biol. Chem. **279**:51305–51314.

37. **Schader SM, Colby-Germinario SP, Quashie PK, Oliveira M, Ibanescu RI, Moisi D, Mespléde T, Wainberg MA.** 2012. HIV gp120 H375 is unique to HIV-1 subtype CRF01_AE and confers strong resistance to the entry inhibitor BMS-599793, a candidate microbicide drug. Antimicrob. Agents Chemother. **56**:4257–4267.

38. **Ferguson SM, De Camilli P.** 2012. Dynamin, a membrane-remodelling GTPase. Nat. Rev. Mol. Cell Biol. **13**:75–88.

39. **Carter GC, Bernstone L, Baskaran D, James W.** 2011. HIV-1 infects macrophages by exploiting an endocytic route dependent on dynamin, Rac1 and Pak1. Virology **409**:234–250.

40. **Pritschet K, Donhauser N, Schuster P, Ries M, Haupt S, Kittan NA, Korn K, Pöhlmann S, Holland G, Bannert N, Bogner E, Schmidt B.** 2012. CD4- and dynamin-dependent endocytosis of HIV-1 into plasmacytoid dendritic cells. Virology **423**:152–164.

41. **Joshi S, Braithwaite AW, Robinson PJ, Chircop M.** 2011. Dynamin inhibitors induce caspase-mediated apoptosis following cytokinesis fail-

ure in human cancer cells and this is blocked by Bcl-2 overexpression. Mol. Cancer **10**:78.

42. **Quan A, McGeachie AB, Keating DJ, van Dam EM, Rusak J, Chau N, Malladi CS, Chen C, McCluskey A, Cousin MA, Robinson PJ.** 2007. Myristyl trimethyl ammonium bromide and octadecyl trimethyl ammonium bromide are surface-active small molecule dynamin inhibitors that block endocytosis mediated by dynamin I or dynamin II. Mol. Pharmacol. **72**:1425–1439.

43. **Engel S, Heger T, Mancini R, Herzog F, Kartenbeck J, Hayer A, Helenius A.** 2011. Role of endosomes in simian virus 40 entry and infection. J. Virol. **85**:4198–4211.

44. **Fra AM, Williamson E, Simons K, Parton RG.** 1994. Detergent-insoluble glycolipid microdomains in lymphocytes in the absence of caveolae. J. Biol. Chem. **269**:30745–30748.

45. **Harris J, Werling D, Hope JC, Taylor G, Howard CJ.** 2002. Caveolae and caveolin in immune cells: distribution and functions. Trends Immunol. **23**:158–164.

46. **Hatanaka M, Maeda T, Ikemoto T, Mori H, Seya T, Shimizu A.** 1998. Expression of caveolin-1 in human T cell leukemia cell lines. Biochem. Biophys. Res. Commun. **253**:382–387.

47. **Vallejo J, Hardin CD.** 2005. Expression of caveolin-1 in lymphocytes induces caveolae formation and recruitment of phosphofructokinase to the plasma membrane. FASEB J. **19**:586–587.

48. **McMahon HT, Boucrot E.** 2011. Molecular mechanism and physiological functions of clathrin-mediated endocytosis. Nat. Rev. Mol. Cell Biol. **12**:517–533.

49. **Ivanov AI.** 2008. Pharmacological inhibition of endocytic pathways: is it specific enough to be useful? Methods Mol. Biol. **440**:15–33.

50. **Heuser JE, Anderson RG.** 1989. Hypertonic media inhibit receptor-mediated endocytosis by blocking clathrin-coated pit formation. J. Cell Biol. **108**:389–400.

51. **von Kleist L, Haucke V.** 2012. At the crossroads of chemistry and cell biology: inhibiting membrane traffic by small molecules. Traffic **13**:495–504.

52. **Fredericksen BL, Wei BL, Yao J, Luo T, Garcia JV.** 2002. Inhibition of endosomal/lysosomal degradation increases the infectivity of human immunodeficiency virus. J. Virol. **76**:11440–11446.

53. **Wei BL, Denton PW, O'Neill E, Luo T, Foster JL, Garcia JV.** 2005. Inhibition of lysosome and proteasome function enhances human immunodeficiency virus type 1 infection. J. Virol. **79**:5705–5712.

54. **Bayer N, Schober D, Prchla E, Murphy RF, Blaas D, Fuchs R.** 1998. Effect of bafilomycin A1 and nocodazole on endocytic transport in HeLa cells: implications for viral uncoating and infection. J. Virol. **72**:9645–9655.

55. **Lusso P, Cocchi F, Balotta C, Markham PD, Louie A, Farci P, Pal R, Gallo RC, Reitz MS.** 1995. Growth of macrophage-tropic and primary human immunodeficiency virus type 1 (HIV-1) isolates in a unique CD4$^+$ T-cell clone (PM1): failure to downregulate CD4 and to interfere with cell-line-tropic HIV-1. J. Virol. **69**:3712–3720.

56. **Anantharam A, Bittner MA, Aikman RL, Stuenkel EL, Schmid SL, Axelrod D, Holz RW.** 2011. A new role for the dynamin GTPase in the regulation of fusion pore expansion. Mol. Biol. Cell **22**:1907–1918.

57. **Sun Y, Tien P.** 2013. From endocytosis to membrane fusion: emerging roles of dynamin in virus entry. Crit. Rev. Microbiol. **39**:166–179.

58. **Liu L, Oliveira NM, Cheney KM, Pade C, Dreja H, Bergin AM, Borgdorff V, Beach DH, Bishop CL, Dittmar MT, McKnight A.** 2011. A whole genome screen for HIV restriction factors. Retrovirology **8**:94. doi:10.1186/1742-4690-8-94.

59. **Harrison IP, McKnight A.** 2011. Cellular entry via an actin and clathrin-dependent route is required for Lv2 restriction of HIV-2. Virology **415**:47–55.

60. **Lu J, Pan Q, Rong L, He W, Liu SL, Liang C.** 2011. The IFITM proteins inhibit HIV-1 infection. J. Virol. **85**:2126–2137.

61. **Schoggins JW, Wilson SJ, Panis M, Murphy MY, Jones CT, Bieniasz P, Rice CM.** 2011. A diverse range of gene products are effectors of the type I interferon antiviral response. Nature **472**:481–485.

62. **Del Portillo A, Tripodi J, Najfeld V, Wodarz D, Levy DN, Chen BK.** 2011. Multiploid inheritance of HIV-1 during cell-to-cell infection. J. Virol. **85**:7169–7176.

63. **Gobeil LA, Lodge R, Tremblay MJ.** 2013. Macropinocytosis-like HIV-1 internalization in macrophages is CCR5-dependent and leads to efficient but delayed degradation in endosomal compartments. J. Virol. **87**:735–745.

64. **Permanyer M, Ballana E, Esté JA.** 2010. Endocytosis of HIV: anything goes. Trends Microbiol. **18**:543–551.

65. **Zhong P, Agosto LM, Ilinskaya A, Dorjbal B, Truong R, Derse D, Uchil PD, Heidecker G, Mothes W.** 2013. Cell-to-cell transmission can overcome multiple donor and target cell barriers imposed on cell-free HIV. PLoS One **8**:e53138. doi:10.1371/journal.pone.0053138.

66. **Maréchal V, Prevost MC, Petit C, Perret E, Heard JM, Schwartz O.** 2001. Human immunodeficiency virus type 1 entry into macrophages mediated by macropinocytosis. J. Virol. **75**:11166–11177.

67. **Gobeil LA, Lodge R, Tremblay MJ.** 2012. Differential HIV-1 endocytosis and susceptibility to virus infection in human macrophages correlate with the cell activation status. J. Virol. **86**:10399–10407.

68. **Vasiliver-Shamis G, Dustin ML, Hioe CE.** 2010. HIV-1 virological synapse is not simply a copycat of the immunological synapse. Viruses **2**:1239–1260.

69. **Davis DM.** 2007. Intercellular transfer of cell-surface proteins is common and can affect many stages of an immune response. Nat. Rev. Immunol. **7**:238–243.

70. **Abela IA, Berlinger L, Schanz M, Reynell L, Günthard HF, Rusert P, Trkola A.** 2012. Cell-cell transmission enables HIV-1 to evade inhibition by potent CD4bs directed antibodies. PLoS Pathog. **8**:e1002634. doi:10.1371/journal.ppat.1002634.

71. **Durham ND, Yewdall AW, Chen P, Lee R, Zony C, Robinson JE, Chen BK.** 2012. Neutralization resistance of virological synapse-mediated HIV-1 infection is regulated by the gp41 cytoplasmic tail. J. Virol. **86**:7484–7495.

72. **Massanella M, Puigdomènech I, Cabrera C, Fernandez-Figueras MT, Aucher A, Gaibelet G, Hudrisier D, García E, Bofill M, Clotet B, Blanco J.** 2009. Anti-gp41 antibodies fail to block early events of virological synapses but inhibit HIV spread between T cells. AIDS **23**:183–188.